

# First-principles Simulations of the stretching and final breaking of Al nanowires: Mechanical properties and electrical conductance

Pavel Jelínek<sup>1,2</sup>, Rubén Pérez<sup>1</sup>, José Ortega<sup>1</sup> and Fernando Flores<sup>1</sup>

<sup>1</sup> Departamento de Física Teórica de la Materia Condensada,  
Universidad Autónoma de Madrid, E-28049 Spain and

<sup>2</sup> Institute of Physics, Academy of Sciences of the Czech Republic,  
Čukrovarnická 10, 1862 53, Prague, Czech Republic

(Dated: March 22, 2024)

The evolution of the structure and conductance of an Al nanowire subject to a tensile stress has been studied by first-principles total-energy simulations. Our calculations show the correlation between discontinuous changes in the force (associated to changes in the bonding structure of the nanowire) and abrupt modifications of the conductance as the nanowire develops a thinner neck, in agreement with the experiments. We reproduce the characteristic increase of the conductance in the last plateau, reaching a value close to the conductance quantum  $G_0 = 2e^2/h$  before the breaking of the nanowire. A dimmer describes the contact geometry at these last stages, with three channels (one dominant) contributing to the conductance.

PACS numbers: 73.63.bj, 62.25.+g, 73.63.Rt, 68.65.-k

The electrical and mechanical properties of metallic nanowires have received a lot of attention [1]. Although point contacts have been studied for many years, only recently the gentle control of the distance between two metals using an STM-AFM [2] or a mechanically controlled breaking junction (MCBJ) [3] has allowed the experimental characterization of atomic contacts and the observation of quantum effects in both the conductance and the forces [2]. In a pioneering work, Scheer et al. [4] have shown, analyzing the superconducting properties of an atomic contact, how the transport properties of the system just before the breaking point depend on a few channels that they related to the atomic orbitals of the contact.

The formation of necks and atomic contacts in stretched metallic nanowires has been analyzed theoretically using different approaches. The nanowire deformation can be studied by molecular dynamics simulations using either classical [5, 6] or effective-medium theory potentials [7, 8]. First principles calculations based on Density Functional theory (DFT) [9, 10] provide a more accurate description of the mechanical properties and the electronic structure needed for the calculation of the conductance, but the large computational demand restricts most of the applications to the analysis of model geometries for the contact (e.g. monoatomic chains). Up to our knowledge, the most complete calculation of the deformation of a metallic nanowire has been presented by Nakamura et al. [11], who analyzed, using DFT calculations, a Na nanowire with 39 atoms. In this simulation, the wire is elongated in steps of 0.2 or 0.4 Å until it reaches the breaking point. The conductance is determined using the Landauer-Buttiker formula, where the transmission matrix is calculated from the self-consistent electrostatic potential using scattering techniques [12]. This calculation showed how the nanowire deformation was accompanied

by a rearrangement of the atomic configuration, that introduces also jumps in the forces and the conductance of the system.

Addressing this complex problem with a fully-converged first-principles description would be still too computationally demanding. One possibility is to stick to accurate plane-wave (PW) DFT methods, carefully relaxing the conditions for convergence [13] (basis set cutoff, k-point sampling, etc). A second alternative is to resort to local orbital MD-DFT methods, specially those devised with the aim of computational efficiency, that allow first-principles studies of much more complex systems. The formulation in terms of local orbitals has an added value, as the transport properties can be easily calculated from the resulting (tight-binding or LCAO) electronic hamiltonian using non-equilibrium Green's function techniques [14]. Thus, efficient local orbital MD-DFT methods are probably the best available tools for a first-principles analysis of complex nanowires. In this work, we have studied the evolution of the structure and the conductance of an Al nanowire as a function of the stretching by means of a fast local orbital minimal basis MD-DFT technique (Fireball96) [15]. This technique offers a very favorable accuracy/efficiency balance if the atomic-like basis set is chosen carefully [16]. This approach is complemented with PW-DFT calculations (using CASTEP [18]) performed at the critical points of the nanowire deformation, as discussed below. Closely related approaches [19, 20, 21, 22], based on the combination of ab-initio calculations on local orbital basis and Keldysh-Green function methods, have been recently applied to characterize some ideal geometries (mainly, atomic chains) for Al and Au nanowires.

We have studied the system shown in figure 1A, having 48 atoms {12 of them in the wire}, embedded in an Al(111) surface having a (3x3) periodicity. We also

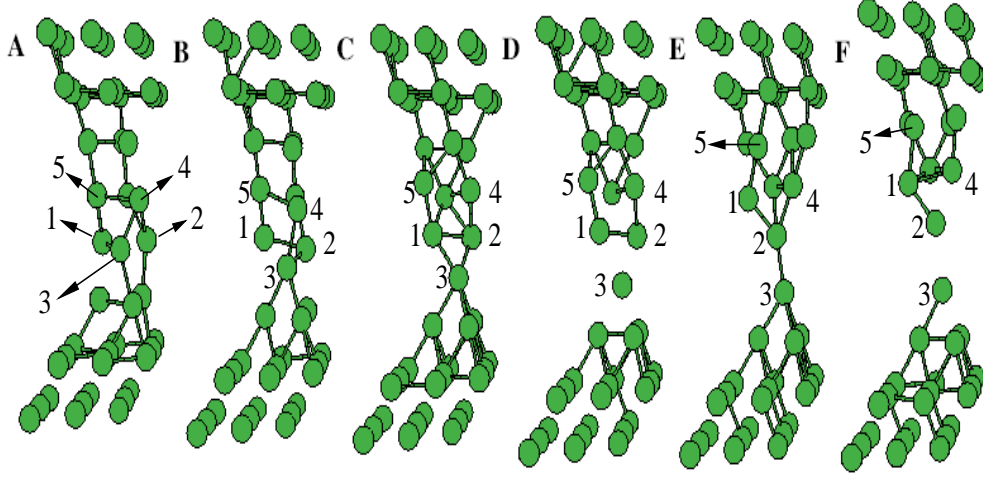


FIG. 1: Ball-and-Stick model of the structure of the Al nanowire for different steps of the stretching process (see Fig. 2). The atoms involved in the important bonding rearrangements related to discontinuous changes in total energy, force and conductance are labelled 1 to 5.

impose periodic conditions in the direction perpendicular to the surface, joining artificially the last two layers of the system. The stretching of the system is simulated increasing the distance between the two limiting layers by steps of 0.1 Å. After each step, the system is allowed to relax toward its configuration of minimum energy; in this relaxation, only the atoms located in the last two layers remain fixed, meaning that 30 atoms are allowed to relax. We have checked the validity of the calculation performed with Fireball96, repeating similar calculations with CASTEP at points of the deformation where rearrangement of the atoms appeared (see the discussion below). Figure 1 shows snapshots of the nanowire geometry along the stretching path; different profiles correspond to the points labelled A to F in Fig. 2, where the total energy per atom is shown as function of the stretching displacement. This figure 2 displays the points where the nanowire suffers an important rearrangement in its geometry: these jumps occur between points B and C, and between points D and E. Fig. 1 shows the initial geometry (A), the geometries before and after the first (B,C) and second (D,E) jumps, and the structure close to the final breaking point (F). It is important to notice that the main rearrangement of atoms occurs in the layer formed by atoms 1, 2 and 3. In particular, along the path AB, the atom 3 starts to move out of the initial 1-2-3 layer; at the first jump, this atom takes an independent position linking a lower layer and the two atoms 1-2. Along the path CD, the geometry of the point C does not change too much, the atom 2 moving slowly toward atom 3; eventually, at the second jump, atom 2 forms a dimer with atom 3, and the nanowire reaches a geometry very similar to the one formed at the breaking point. In particular, along the EF path the system evolves basically

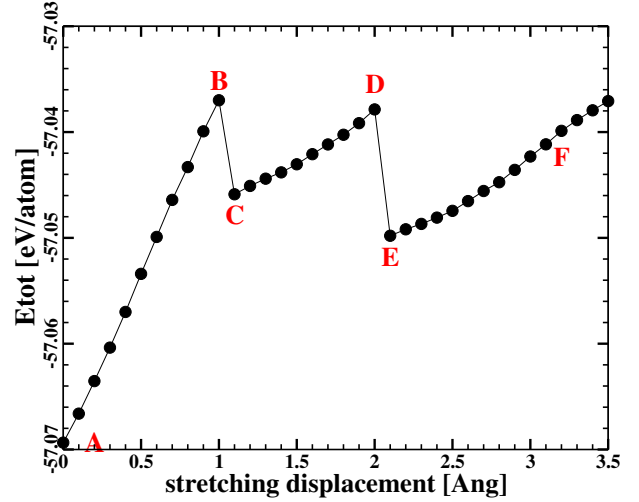


FIG. 2: Total energy of the Al nanowire as a function of the stretching displacement,  $d$ .

changing mostly the distance between atoms 2 and 3.

We have checked these calculations, obtained using a Fireball code, by recalculating geometries around the jumps (BC and DE) using CASTEP: these calculations confirm the validity of the Fireball results; we have found, however, some minor differences. For instance, in CASTEP we find the system to present the first jump for  $d = 0.9$  Å, namely, a step before the jump found in Fireball; the system evolves, however, across the first jump to the same geometry calculated in Fireball.

Figure 3 shows the force along the nanowire stretching. It is very satisfactory that the first jump seems to appear for a maximum in the force; along the path CD the force

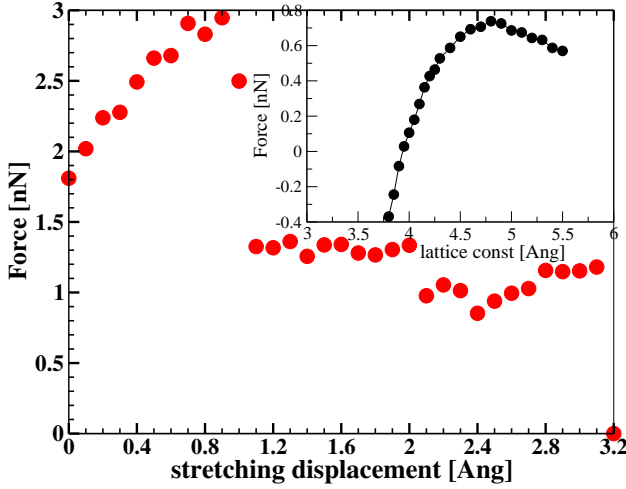


FIG. 3: Normal force along the stretching path. The inset shows the force between n.n. atoms in Al crystal defined as the derivative of the energy per atom with respect to the n.n. distance during hydrostatic strain, divided by 6 bonds assumed in the f.c.c. structure.

is practically constant and along the normal deformation, path EF, the force increases except for some small fluctuations, until reaching a maximum at the point where the wire breaks. It is interesting to compare the forces shown in 3, with the one calculated at the break point for an Al-crystal: this is defined by the maximum derivative of the energy per atom with respect to the nearest-neighbor distance for an Al-crystal, divided by the number of bonds each atom is assumed to form (6 bonds per atom in a f.c.c. structure). Our calculations yield 0.7 nN for the maximum force, and this quantity should be compared with the forces of Fig. 3 that are typically larger than that value: at the nanowire break point the force is around 1.2 nN, 1.7 times the bulk value.

We have calculated the electrical conductance of the nanowire using a Keldysh-Green function approach based on the first-principles tight-binding Hamiltonian obtained from the Fireball code, at each point of the deformation path. In this formalism, we rewrite this Hamiltonian describing the system as  $\hat{H}_1 + \hat{H}_2 + \hat{T}_{12}$ , where the total system is splitted into the two parts, 1 and 2,  $\hat{T}_{12}$  dening the coupling between both. Typically, we use the thinnest part of the nanowire to define the interface between these two subsystems. Then, the differential conductance [14] is given by:

$$G = \frac{dI}{dV} = \frac{4e}{h} \text{Im Tr } \hat{T}_{12} \hat{G}_{22}^r(E_F) \hat{D}_{22}^r(E_F) \hat{T}_{12} \hat{G}_{11}^r(E_F) \hat{D}_{11}^a(E_F) \quad (1)$$

where  $\hat{G}_{11}$  and  $\hat{G}_{22}$  are the density matrices associated with sides 1 and 2, respectively, while:

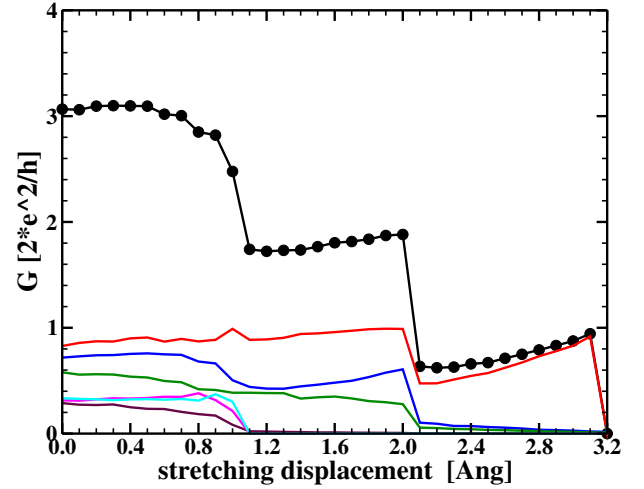


FIG. 4: Total differential conductance (in units of the conductance quantum) and channel contribution along the stretching path.

$$\hat{D}_{22}^r = [\hat{1} - \hat{T}_{12} \hat{G}_{22}^r(E_F) \hat{T}_{21} \hat{G}_{11}^r(E_F)]^{-1} \quad (2)$$

and  $\hat{D}_{11}^a$  is given by a similar eqn.;  $\hat{G}_{11}^r$  and  $\hat{G}_{22}^r$  are the retarded Green function of the decoupled sides, 2 and 1.

Using eqn. 1, we calculate the differential conductance along the stretching deformation (Fig. 4). From this figure we see how this conductance changes dramatically at the points B-C and D-E: in both cases the conductance jump coincides with the force jump (Fig. 3), and is determined by the atomic rearrangement the system suffers at those points. The conductance behavior shows two other important features: (i) the nanowire breaks at a point where the conductance is very close to the quantum unit,  $G \approx 0.95 \frac{2e^2}{h}$ ; (ii) second, before the breaking point, the conductance takes values a little smaller than the last one, with a negative slope. These two features are in good agreement with the experimental evidence [1, 23]. Moreover, at the breaking point the system shows a geometry slightly different to the one suggested in [4]. In particular, we find that an Al-dimer is responsible for the conductance properties the nanowire shows before it breaks.

Finally, we have also addressed the question of how many different channels contribute to the conductance. This has also been analyzed using eqn. 1; this eqn. can be rewritten, using the cyclic property of the trace in the form:

$$G = \frac{dI}{dV} = \frac{4e}{h} \text{Im Tr } (\hat{t} \hat{t}^\dagger); \quad (3)$$

where  $\hat{t} = \hat{G}_{11}^a \hat{D}_{11}^a \hat{T}_{12} \hat{G}_{22}^a$  [24]. By diagonalizing this trans-

fer matrix, we find the channels contributing to  $G$ .

Figure 4 also shows how different channels contribute to the total differential conductance. Near the break point, we find that only three channels yield appreciable contributions to the total current, although there appears a predominant mode, very much in agreement with the results published by Scheer et al [4]. Along the trajectory CD, before the last jump, the system also presents three predominant channels, but, in this case, all the three yield important contributions to the current; notice that in this case, the total conductance is around  $2 \frac{2e^2}{h}$ , with a channel contributing practically  $\frac{2e^2}{h}$ , and two other channels, each one contributing  $\frac{1}{2} \frac{2e^2}{h}$ . In the initial path, AB in Fig 1, we find six channels contributing with a total conductance of around  $3 \frac{2e^2}{h}$ . From this analysis we conclude that the channels are not either open or closed; their particular contribution depends very much on the geometry of the nanowire contact. We can only say that channels tend to close along the nanowire deformation, and that once a channel is closed by the stretching deformation it remains closed all the time.

In conclusion, we have presented total energy DFT calculations for the stretching deformation of an Al-nanowire. The use of a fast local-orbital code has allowed us to analyze in detail the nanowire geometrical configurations along the stretching path. At the same time, the first-principles tight-binding Hamiltonian obtained at each geometry for the electronic system, has allowed us to analyze also in a very efficient way, using Keldish-Green function methods, the differential conductance of the system. Our results reproduce most of the experimental evidence, and show that the deformation induces at particular points sudden rearrangement of atoms that manifest itself in jumps of the forces and the conductance. We also find that in the final process of deformation, the nanowire breaks at a point having a differential conductance close to  $\frac{2e^2}{h}$ , and that the total conductance is the result of the contribution of three channels, one of them being the predominant one.

P.J. gratefully acknowledges financial support by the

European project no. HPRN-CT-2000-00154. This work has been supported by the DG I+D+CyT (Spain) under contract MAT2001-0665, and by Consejería de Educacion de la Comunidad de Madrid under project 07N/0050/2001.

- 
- [1] N. Agraït, A. Levy-Yeyati, J. van Ruitenbeek, cond-mat/0208239 (2002).
  - [2] G. Rubio, N. Agraït, S. Vieira Phys. Rev. Lett 76, 2302 (1996).
  - [3] E. Scheer et al, Phys. Rev. Lett. 78, 3535 (1997).
  - [4] E. Scheer et al, Nature 394, 154 (1998).
  - [5] U. Landman et al, Phys. Rev. Lett 77, 1362 (1996).
  - [6] T.N. Todorov, A.P. Sutton, Phys. Rev. Lett 70, 2138 (1993).
  - [7] A.M. Bratkovsky, A.P. Sutton, T.N. Todorov, Phys. Rev. B 52, 5036 (1995).
  - [8] M.R. Sorensen, M. Brandbyge, K.W. Jacobsen, Phys. Rev. B 57, 3283 (1998).
  - [9] N.D. Lang, Phys. Rev. B 52, 5335 (1995).
  - [10] N. Kobayashi, M. Brandbyge, M. Tsukada, Phys. Rev. B 62, 8430 (2000).
  - [11] A. Nakamura et al, Phys. Rev. Lett. 82, 1538 (1999).
  - [12] K. Hirose and M. Tsukada, Phys. Rev. B 51, 5278 (1995).
  - [13] D. Kugler et al, Phys. Rev. Lett. 89, 186402 (2002).
  - [14] N. Mingo et al, Phys. Rev. B 54, 2225 (1996).
  - [15] A. Demkov et al, Phys. Rev. B 52, 1618 (1995).
  - [16] The valence electrons were described by s and p slightly excited pseudoatomic orbitals [17]. For the cutoff radii  $R_c = 6.4a.u$ : we obtained for fcc Al a lattice parameter of  $a = 3.97 \text{ \AA}$  and a bulk modulus of  $B = 74 \text{ GPa}$  (experiment:  $a = 4.05 \text{ \AA}$ ,  $B = 76 \text{ GPa}$ ).
  - [17] O.F. Sankey, D.J. Niklewski, Phys. Rev. B 40, 3979 (1989).
  - [18] CASTEP 4.2 Academic version, licensed under the UKCP-MSI Agreement, 1999. M.C. Payne et al, Rev. Mod. Phys. 64, 1045 (1992).
  - [19] G. Taraschi et al, Phys. Rev. B 58, 13138 (1998).
  - [20] H. Mehrez et al, Phys. Rev. B 65, 195419 (2002).
  - [21] M. Brandbyge et al, Phys. Rev. B 65, 165401 (2002).
  - [22] J.J. Palacios et al, Phys. Rev. B 66, 35322 (2002).
  - [23] J.C. Cuevas et al, Phys. Rev. Lett. 81, 2990 (1998).
  - [24] M. Buttiker et al, Phys. Rev. B 31, 6207 (1985).